Temperature dependence of nuclear spin coherence in Eu^{3+}:Y_2SiO_5

Andrea Arcangeli,[1,2,*] Roger M. Macfarlane,[3] Alban Ferrier,[1,4] and Philippe Goldner[1]

[1]*PSL Research University, Chimie ParisTech—CNRS, Institut de Recherche de Chimie Paris, 75005 Paris, France*

[2]*NEST, Scuola Normale Superiore and Istituto Nanoscienze-CNR, Piazza San Silvestro 12, 56127 Pisa, Italy*

[3]*IBM Almaden Research Center, 650 Harry Road, San Jose, California 95120, USA*

[4]*Sorbonne Universités, UPMC Université Paris 06, 75005, Paris, France*

(Received 3 July 2015; revised manuscript received 16 October 2015; published 1 December 2015)

We have measured the temperature dependence of the spin-lattice relaxation and dephasing of the two nuclear quadrupole transitions in the $^7F_0$ ground state of ^{151}Eu in yttrium orthosilicate up to 21 K. Spin-lattice relaxation (T_1) is dominated by an Orbach process and decoherence comes from ^{87}Y nuclear spin fluctuations at low temperatures and is T_1 limited at higher temperatures. The different contributions to relaxation and dephasing are evaluated.

DOI: 10.1103/PhysRevB.92.224401 PACS number(s): 76.60.Gv, 76.30.Kg, 76.60.Lz, 76.70.Hb

I. INTRODUCTION

Nuclear spin transitions of rare earth ions are becoming the subject of growing interest in the field of quantum information (QI) technology [1–4]. This is in part due to their long coherence lifetimes at low temperature (around 2–3 K), that were recently demonstrated to exceed 6 h under certain conditions [5], combined with the possibility of optical manipulation [6–8].

Most experimental demonstrations of QI, such as quantum memories and teleportation, have been performed at low T (<2 K) [9–13], where phonon-induced dephasing is negligible. It would be technologically desirable to be able to implement QI applications at elevated temperatures. Materials for high-temperature QI applications have been proposed [14–18], but systems preserving both long coherence times and optical properties suitable for light storage at temperatures significantly above 4 K remain elusive.

We present here the measurement of the temperature dependence of rare earth nuclear spin coherence at temperatures well above that of liquid helium, up to 21 K. We find that usefully long coherence times of several milliseconds (ms) can be obtained in Eu^{3+}-doped Y_2SiO_5 (YSO). Rare-earth-doped YSO has been suggested as one of the most promising materials for the next generation of quantum memories and repeaters [9,10,13,19–21], often with Eu^{3+} as the dopant ion [22–24]. Eu^{3+} hyperfine structure could provide tens of megahertz (MHz) of optical bandwidth for memories while ground-state nuclear coherence can be extended and controlled by magnetic [5] or electric [25] fields.

To measure the temperature dependence of the spin relaxation of the hyperfine transitions, we used Raman heterodyne detection of nuclear quadrupole resonance (NQR) [26,27]. This technique is ideally suited to study open-shell systems with narrow optical transitions and hyperfine structure consisting of energy levels spaced by tens of MHz. The technique is not very demanding in terms of laser stability or power, and the excitation of spin states is provided by readily available coherent rf sources. We measured spin-lattice relaxation (T_1) and spin dephasing (T_2) up to 21 K, extending the range covered in the literature for this system and providing a measurement of the temperature dependence of T_2. The relatively long decoherence time of 3.3 ms at 21 K makes this material compatible with interesting QI-related applications at elevated temperatures.

II. EXPERIMENTAL METHODS

The investigated sample was a $1 \times 2.5 \times 5\,\mathrm{mm}^3$, Czochralski-grown 0.1 at.% Eu^{3+}-doped Y_2SiO_5 single crystal with natural ^{151}Eu abundance (44.77%). It has been shown [28] that the optical coherence times are insensitive to Eu^{3+} concentration in the range 0.02%–1%. Y_2SiO_5 is monoclinic, with cell parameters $a = 1.041\,\mathrm{nm}$, $b = 0.6721\,\mathrm{nm}$, $c = 1.249\,\mathrm{nm}$, and $\beta = 102^\circ 39'$. The crystal belongs to the C_{2h}^6 space group and has eight formula units in a unit cell. Eu^{3+} ions substitute for Y^{3+} in two crystallographically inequivalent sites of C_1 symmetry. The crystal is biaxial, with the optical normal along the b axis and the other two principal axes ($D1$ and $D2$) in the a-c plane. The sample was cut along the $D1$, $D2$, and b axes. The light, propagating parallel to the b crystal axis, was polarized along $D1$ in order to maximize the absorption. All the measurements refer to $^{151}Eu^{3+}$ in crystallographic site 1 [29]. Helmholtz coils were used to apply magnetic fields up to 80 G along $D1$. The crystal was mounted in a Janis optical helium bath cryostat with a temperature sensor attached directly to the surface of the sample by thermally conducting grease. To keep the temperature constant during the time of the measurements we used a proportional-integral-derivative (PID) controlled heating system and a fine control of helium flow. In this way we could stabilize the temperature to 0.5 K over 1 h. The rf pickup in the PID system was the main limiting factor to the temperature stability. The technique used for the investigation of the ground-state hyperfine transitions in Eu^{3+} is the Raman heterodyne detection of NQR [26,27], which allows for direct excitation of the hyperfine transitions by an rf field and optical detection of the coherence via resonant scattering through an optical excited state—here the $^5D_0$ level of Eu^{3+} in site 1 of Y_2SiO_5 at $17\,240.2\,\mathrm{cm}^{-1}$. Rf excitation was delivered to the sample by a 6-mm-diameter, 1.5-cm-long silvered oxygen-free copper coil. The rf waveforms were generated by an Agilent N8242A arbitrary waveform generator and for pulsed experiments, the rf current

*andrea.arcangeli@nano.cnr.it

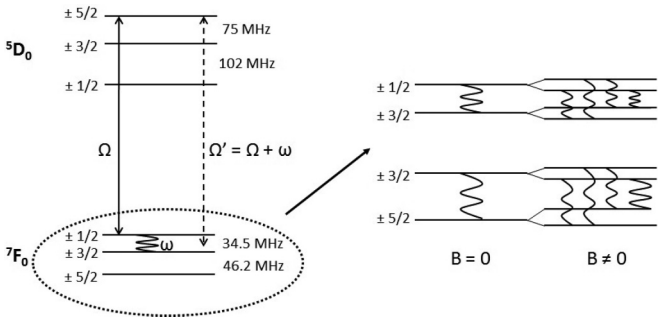

FIG. 1. Energy level structure of $^{151}Eu^{3+}$:Y_2SiO_5 in zero magnetic field and in an external field B. The $^7F_0 \rightarrow {}^5D_0$ optical transition is located at 17 240.2 cm^{-1} for $^{151}Eu^{3+}$ in site 1. The figure shows one of the Raman transitions that contribute to the signal for the 34.5 MHz coherence.

in the coil was enhanced by lumped element resonant circuits. The maximum available rf power dissipated in a 50-Ω load was 150 W. Optical transitions were excited by a Coherent 899-21 ring dye laser operating with Rhodamine 6G, and a linewidth of ∼1 MHz. The frequency and intensity of the laser beam were controlled by acousto-optic modulators mounted in a double-pass configuration. The laser also serves as a local oscillator for the detection of the beating with the coherent field emitted in the same spatial mode from the sample at a frequency $\Omega' = \Omega + \omega$, where Ω is the frequency of the laser and ω is the frequency difference between the hyperfine levels involved in the transition (Fig. 1). In our pumping scheme all optical transitions are excited simultaneously, and the signal

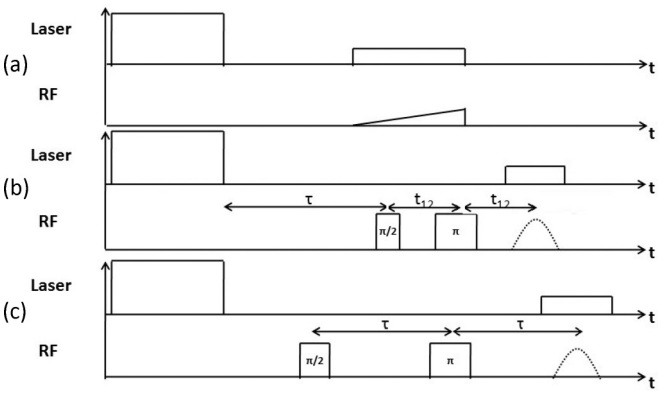

FIG. 2. Optical and rf sequences used for the different experiments. Straight lines represent constant frequencies, sloping lines frequency sweeps. The first rectangle in the laser axes represents the optical pumping employed to obtain a nonthermal population distribution within the spin states. This consists of a series of strong (≈10 mW) chirped optical pulses, burning a 10-MHz-wide hole around the probe frequency. The spin echoes are sketched as dotted lines. (a) Measurement of the hyperfine spectra: The rf is swept across the transition while a weak optical probe is on. (b) T_1 measurement: The delay between the optical pumping and the rf echo sequence is changed while keeping constant the rf pulse separation t_{12} (200 μs). The optical probe is on during the echo emission. (c) Coherence time measurement: The time interval τ between the pulses is varied and a decay of the echo signal is recorded. The optical probe is on during the echo emission.

is formed by the phase-sensitive detection of the rf-excited hyperfine transitions. The optical signal was detected by a Thorlabs PDB150A photodiode, demodulated, amplified by low-noise amplifiers and recorded by a digital oscilloscope. An overview of the rf and optical excitation and detection sequences, described later in the paper, is given in Fig. 2.

III. RESULTS AND DISCUSSION

A. $^7F_0$ hyperfine structure

The spectra of the $I_z = \pm 1/2 \leftrightarrow \pm 3/2$ and $I_z = \pm 3/2 \leftrightarrow \pm 5/2$ transitions centered, respectively, at 34.54 and 46.17 MHz were measured at 4 K. The results are shown in Fig. 3. In both cases, a small static magnetic field (up to ≈80 G) was applied along $D1$, removing the state degeneracy along the quantization axis. The relatively large (38 kHz [23]) inhomogeneous linewidth of the $I_z = \pm 3/2 \leftrightarrow \pm 5/2$ transition and the small γ value of 1.1 kHz/G did not allow full separation of the four lines, leading to an incompletely resolved spectrum. The $I_z = \pm 1/2 \leftrightarrow \pm 3/2$ transitions, on the other hand, could be completely resolved. The width of the lines shown in Fig. 3 might be affected by some additional broadening due to a slight misalignment of the magnetic field with respect to $D1$. This is due to the nonequivalence under the application of an external field of the two sub-sites in which Eu^{3+} ions replace Y in Y_2SiO_5 [30]. The signal was observed using a weak optical probe (≈1 mW) while scanning with 4 W of rf across the transitions [Fig. 2(a)]. The knowledge of the transition energies was used to tune the rf resonant circuits to 34.58 MHz and 46.22 MHz for the following experiments. In this way, we were able to efficiently drive the transitions using rf pulses corresponding to relatively high Rabi frequencies, of ≈100 kHz, larger than the inhomogeneous width of the driven transitions.

B. T_1 measurement

The relaxation dynamics of the spin states were investigated by an inversion-recovery-like technique. A nonthermal population distribution was first created by optical pumping; then a standard spin-echo sequence consisting of closely

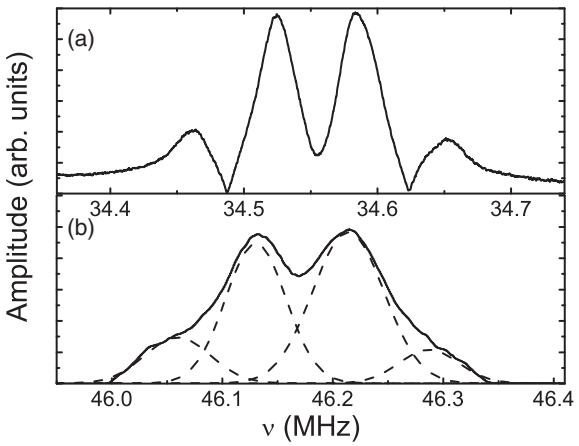

FIG. 3. Spectra of the $^7F_0$ ground-state hyperfine transitions of $^{151}Eu^{3+}$:Y_2SiO_5 in a static magnetic field. (a) $I_z = \pm 1/2 \rightarrow \pm 3/2$ ($B = 48$ G) and (b) $I_z = \pm 3/2 \rightarrow \pm 5/2$ ($B = 80$ G). The dashed line shows a deconvolution of the unresolved spectrum.

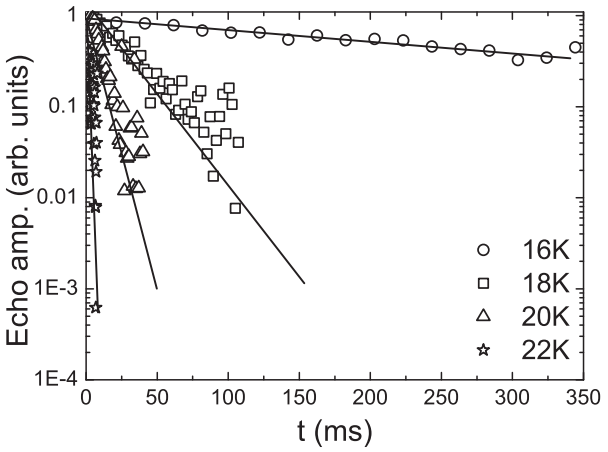

FIG. 4. T_1 measurement: decay of the echo amplitude for different time delays t between optical pumping and echo sequence measured at different temperatures. The data refer to the $I_z = \pm 1/2 \rightarrow \pm 3/2$ transition (34.5 MHz).

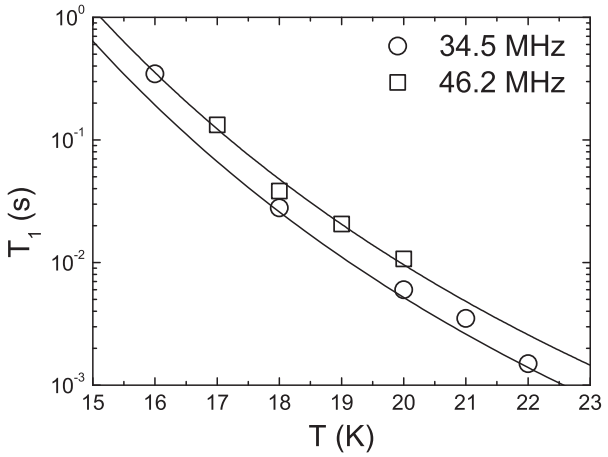

FIG. 5. Temperature dependence of T_1 for the two ground-state hyperfine transitions. The solid lines are a fit to the data using Eq. (1).

spaced (200 μs) $\pi/2$–π pulses was applied to the system. The corresponding rf and laser sequences are shown in Fig. 2(b). In Raman heterodyne scattering, the detected signal is proportional to the population difference between the investigated levels, so a decrease of the measured echo amplitude at different time delays between the optical preparation step and the echo sequence gives a direct measurement of the spin relaxation time T_1. The time resolution of this technique is ultimately given by the separation of the two pulses of the echo sequence. We do not expect significant spectral diffusion effects on the optical transition, as the Eu^{3+} concentration was low [28] and the hole burnt by optical pumping was several MHz wide.

Previous optical hole decay studies showed hole lifetimes on the order of 1 min at relatively high temperature, around 12 K [28]. Although these measurements may result from a combination of the different population decay rates among the three quadrupole levels, they are a good indication of the ground-state spin T_1. We focused on temperatures between 16 and 22 K, extending the range investigated by Könz *et al.* [28]. We separately measured the decay rates of the two ground-state transitions, namely $I_z = \pm 1/2 \leftrightarrow \pm 3/2$ and $I_z = \pm 3/2 \leftrightarrow \pm 5/2$. The experimental curves were obtained by averaging the echo signals over 150 shots. The decays were singly exponential (some are shown as examples in Fig. 4) and the fitted decay time constants are plotted together in Fig. 5. The main relaxation mechanisms giving rise to the temperature dependence of nuclear spin states in solids are the Orbach process [31] and inelastic Raman scattering of phonons [32]. Direct absorption of a single phonon between the individual quadrupole levels is negligible because of the low phonon density of states at these frequencies. The relaxation rate due to the Orbach process is proportional to the phonon occupation number $n(\Delta E)$ at the energy ΔE corresponding to the $^7F_0$-$^7F_1$ transition. Raman scattering of phonons typically exhibits T^7 behavior. As already observed in [28], the main contribution to the spin-lattice relaxation at temperatures above 12 K is given by the Orbach process. Therefore we neglect the Raman term and for the temperature range investigated here we describe the phonon-induced transition broadening as

$$\Gamma_{\text{Orbach}} = A/[e^{(\Delta E/kT)} - 1], \tag{1}$$

where A is a constant describing the strength of the processes. We set the value of ΔE in Eq. (1) to 201 cm^{-1} according to [28], and obtain the Orbach coefficients: $A_{34.5} = 3.7 \times 10^8$ Hz and $A_{46.2} = 2 \times 10^8$Hz for the $I_z = 1/2 \leftrightarrow \pm 3/2$ and $I = \pm 3/2 \leftrightarrow \pm 5/2$ transitions, respectively.

C. Decoherence (T_2) measurement

We investigated the homogeneous linewidth of the ground-state hyperfine transitions as a function of temperature up to 21 K via spin-echo decay measurements. The corresponding rf and optical sequences are described in Fig. 2(c). The decays were measured by increasing the delay between the rf pulses, 100 data points were taken for each decay, and each echo signal was averaged over 200 shots at a repetition rate of 5 Hz. The decays were not exponential for temperatures below $\approx$12 K, indicating the presence of spectral diffusion caused by the distribution of Y spin fluctuation rates. From these decay curves, we obtained the phase memory time T_M defined as

$$S(\tau) = S_0 \exp -[(2\tau/T_M)^x], \tag{2}$$

where $S(\tau)$ is the amplitude of the spin-echo signal corresponding to a separation τ between the two rf pulses, and x is a stretch parameter [33], varying in our case between 1 and 2 (Fig. 6).

The results of the measurements are shown in Fig. 7. Both transitions present a similar behavior: the coherence time is basically constant, with an average value of 25 ms, up to about 16 K, when the phonon contribution to the dephasing sets in strongly. At 21 K the coherence time reduces to 3.3 ms. From the coherence times, we deduced the homogeneous linewidths ($\Gamma_h = 1/\pi T_2$) of the two transitions [Fig. 8(b)]. At low temperature (<16 K) the constant broadening is caused by interaction with ^{87}Y spins of the matrix, which gives a 14-Hz temperature-independent term. This compares with the low-temperature $^7F_0 \rightarrow {}^5D_0$ optical transition width of $\approx$100 Hz, dominated by the population decay time of the $^5D_0$ level at low temperature and broadened by the same

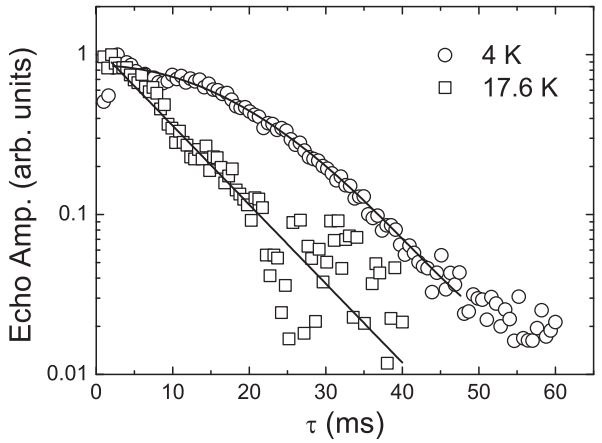

FIG. 6. Echo decay curves at 4 and 17.6 K ($I_z = \pm 1/2 \rightarrow \pm 3/2$ transition) in a magnetic field $B = 60$ G. The solid lines are fits to the experimental data of Eq. (2) for $x = 2$ and $x = 1$, respectively.

thermal process as temperature increases [34] [Fig. 8(a)]. The thermally induced broadening of the nuclear quadrupole levels above 16 K comes from essentially the same process as that of T_1. The Orbach process determining T_1 occurs in two steps: phonon absorption from one quadrupole level to $^7F_1$, followed by phonon emission to a different quadrupole level. The first of those steps can be viewed as a direct process for the homogeneous broadening and has the same magnitude and temperature dependence as the Orbach process. As shown in Fig. 8(b), at higher temperatures, the homogeneous linewidth is T_1 limited, being well described as the sum of the temperature-independent contribution from ^{87}Y spin fluctuations and the T_1 process determined earlier. No additional parameters are required to describe the homogeneous broadening. The crossover between the thermal contribution and the ^{87}Y magnetic contribution to the broadening is at 19 K. Where the homogeneous broadening of the transition is dominated by phonon-induced T_1, techniques commonly used for extending the coherence lifetime of the transitions are expected to be ineffective. These techniques are based on a decoupling of the spin transitions from the surrounding fluctuating magnetic

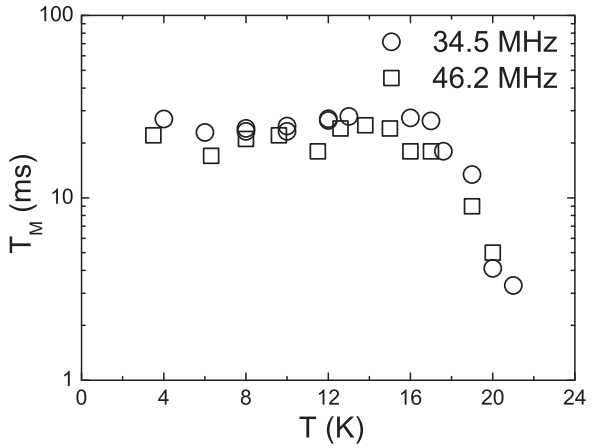

FIG. 7. Phase memory time T_M of the two ground-state hyperfine transitions as a function of temperature in a static magnetic field $B = 60$ G. The reported values are a fit to the experimental data of Eq. (2).

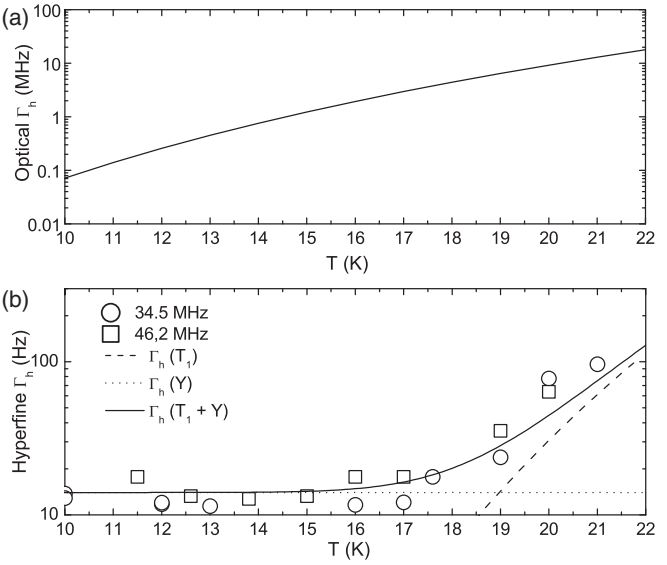

FIG. 8. Temperature dependence of the homogeneous linewidth of the optical (a) and two ground-state hyperfine transitions (b). In (a) the linewidth of the $^7F_0 \rightarrow {}^5D_0$ optical transition is extrapolated from Ref. [28] to the temperature range covered by our experiments. In (b) the dashed line is the T_1 contribution to the broadening, related to the faster of the two hyperfine transitions centered at 34.5 MHz. The dotted line represents a 14-Hz constant term induced by the interaction with ^{87}Y spins in the matrix. The solid line shows the sum of the two previous contributions.

bath of ^{87}Y spins [35,36]. Nevertheless, it is expected that the ^{87}Y flip contribution can be reduced, effectively increasing T_2 up to the T_1 limit. This is particularly interesting in the temperature region where T_1 is still not completely limiting the coherence. If one can eliminate or reduce the 14-Hz broadening induced on the spin transition by ^{87}Y flips, the coherence lifetime is expected to potentially increase up to 1.3 s at 15 K and 22 ms at 19 K. These values represent an upper limit to the achievable coherence lifetime, corresponding to an ideally complete removal of the ^{87}Y magnetic contribution to the dephasing. In addition, no thermal effects on the ^{87}Y magnetic contribution are taken into account. The optical homogeneous linewidth in the same temperature range can be estimated by extending the fit of Könz *et al.* [28] from the low-temperature (<10 K) values. The corresponding optical widths range from 1.2 MHz at 15 K to 6.4 MHz at 19 K [Fig. 8(a)].

IV. CONCLUSION

We investigated the mechanisms that lead to spin-lattice relaxation and spin dephasing in the ground state of Eu^{3+} in Y_2SiO_5 in the 2–21 K temperature range. The experiments were performed by Raman heterodyne detection of nuclear magnetic resonance in the time domain. We measured the spin T_1 for the $I_z = \pm 1/2 \leftrightarrow \pm 3/2$ and $I_z = \pm 3/2 \leftrightarrow \pm 5/2$ ground-state transitions by an inversion-recovery-like technique. An analysis in terms of a resonant Orbach process gives a satisfactory interpretation of the experimental data. Spin-echo decays showed hyperfine coherence times of 25 ms

that were essentially constant between 2 and 16 K. In the same temperature range, spin-lattice relaxation times decrease by a factor of 10^7 [28]. For temperatures above 16 K, T_2 drops rapidly, reaching 7 ms at 19 K and 3.3 ms at 21 K and is essentially T_1 limited. The data presented in this paper show the potential of this system in the field of quantum information storage and processing at elevated temperatures.

ACKNOWLEDGMENTS

This work was supported by the European Union's Seventh Framework Program FP7/2007-2013/ under REA Grant Agreements No. 287252 (CIPRIS, People Program—Marie Curie Actions) and No. 247743 (QuRep) as well as Idex Grant No. ANR-10-IDEX-0001-02 PSL ⋆ and Nano'K project RECTUS.

[1] M. Nilsson, L. Rippe, N. Ohlsson, T. Christiansson, and S. Kröll, Initial experiments concerning quantum information processing in rare-earth-ion doped crystals, Phys. Scr. **T102**, 178 (2002).

[2] A. I. Lvovsky, B. C. Sanders, and W. Tittel, Optical quantum memory, Nat. Photonics **3**, 706 (2009).

[3] J. Wesenberg, K. Mølmer, L. Rippe, and S. Kröll, Scalable designs for quantum computing with rare-earth-ion-doped crystals, Phys. Rev. A **75**, 012304 (2007).

[4] P. Goldner, A. Ferrier, and O. Guillot-Noël, Rare earth-doped crystals for quantum information processing, Handb. Phys. Chem. Rare Earths **46**, 1 (2015).

[5] M. Zhong, M. P. Hedges, R. L. Ahlefeldt, J. G. Bartholomew, S. E. Beavan, S. M. Wittig, J. J. Longdell, and M. J. Sellars, Optically addressable nuclear spins in a solid with a six-hour coherence time, Nature **517**, 177 (2015).

[6] T. E. Northup and R. Blatt, Quantum information transfer using photons, Nat. Photonics **8**, 356 (2014).

[7] M. Gündoğan, M. Mazzera, P. M. Ledingham, M. Cristiani, and H. de Riedmatten, Coherent storage of temporally multimode light using a spin-wave atomic frequency comb memory, New J. Phys. **15**, 045012 (2013).

[8] N. Timoney, B. Lauritzen, I. Usmani, M. Afzelius, and N. Gisin, Atomic frequency comb memory with spin-wave storage in $^{153}Eu^{3+}$:Y_2SiO_5, J. Phys. B: At. Mol. Opt. Phys. **45**, 124001 (2012).

[9] F. Bussières, C. Clausen, A. Tiranov, B. Korzh, V. B. Verma, S. W. Nam, F. Marsili, A. Ferrier, P. Goldner, H. Herrmann, C. Silberhorn, W. Sohler, M. Afzelius, and N. Gisin, Quantum teleportation from a telecom-wavelength photon to a solid-state quantum memory, Nat. Photonics **8**, 775 (2014).

[10] B. Lauritzen, J. Minář, H. de Riedmatten, M. Afzelius, N. Sangouard, C. Simon, and N. Gisin, Telecommunication-wavelength Solid-State Memory at the Single Photon Level, Phys. Rev. Lett. **104**, 080502 (2010).

[11] G. Hetet, J. J. Longdell, A. Alexander, P. Lam, and M. J. Sellars, Electro-Optic Quantum Memory for Light Using Two-Level Atoms, Phys. Rev. Lett. **100**, 023601 (2008).

[12] E. Saglamyurek, N. Sinclair, J. Jin, J. A. Slater, D. Oblak, Bussières, M. George, R. Ricken, W. Sohler, and W. Tittel, Broadband waveguide quantum memory for entangled photons, Nature **469**, 512 (2011).

[13] M. Afzelius, I. Usmani, A. Amari, B. Lauritzen, A. Walther, C. Simon, N. Sangouard, J. Minář, H. de Riedmatten, N. Gisin, and S. Kröll, Demonstration of Atomic Frequency Comb Memory for Light with Spin-Wave Storage, Phys. Rev. Lett. **104**, 040503 (2010).

[14] K. Saeedi, S. Simmons, J. Z. Salvail, P. Dluhy, H. Riemann, N. V Abrosimov, P. Becker, H. Pohl, J. J. L. Morton, and M. L. W. Thewalt, Room-temperature quantum bit storage exceeding 39 minutes using ionized donors in silicon-28, Science **342**, 830 (2013).

[15] K. Bader, D. Dengler, S. Lenz, B. Endeward, S.-D. Jiang, P. Neugebauer, and J. van Slageren, Room temperature quantum coherence in a potential molecular qubit, Nat. Commun. **5**, 5304 (2014).

[16] W. F. Koehl, B. B. Buckley, F. J. Heremans, G. Calusine, and D. D. Awschalom, Room temperature coherent control of defect spin qubits in silicon carbide, Nature **479**, 84 (2011).

[17] G. Balasubramanian, P. Neumann, D. Twitchen, M. Markham, R. Kolesov, N. Mizuochi, J. Isoya, J. Achard, J. Beck, J. Tissler, V. Jacques, P. R. Hemmer, F. Jelezko, and J. Wrachtrup, Ultralong spin coherence time in isotopically engineered diamond, Nat. Mater. **8**, 383 (2009).

[18] N. Bar-Gill, L. M. Pham, A. Jarmola, D. Budker, and R. L. Walsworth, Solid-state electronic spin coherence time approaching one second, Nat. Commun. **4**, 1743 (2013).

[19] M. Gündoğan, P. M. Ledingham, A. Almasi, M. Cristiani, and H. de Riedmatten, Quantum Storage of a Photonic Polarization Qubit in a Solid, Phys. Rev. Lett. **108**, 190504 (2012).

[20] D. Rieländer, K. Kutluer, P. M. Ledingham, M. Gündoğan, J. Fekete, M. Mazzera, and H. de Riedmatten, Quantum Storage of Heralded Single Photons in a Praseodymium-Doped Crystal, Phys. Rev. Lett. **112**, 040504 (2014).

[21] C. Galland, N. Sangouard, N. Piro, N. Gisin, and T. J. Kippenberg, Heralded Single-Phonon Preparation, Storage, and Readout in Cavity Optomechanics, Phys. Rev. Lett. **112**, 143602 (2014).

[22] P. Jobez, I. Usmani, N. Timoney, C. Laplane, N. Gisin, and M. Afzelius, Cavity-enhanced storage in an optical spin-wave memory, New J. Phys. **16**, 083005 (2014).

[23] A. Arcangeli, M. Lovrić, B. Tumino, A. Ferrier, and P. Goldner, Spectroscopy and coherence lifetime extension of hyperfine transitions in $^{151}Eu^{3+}$:Y_2SiO_5, Phys. Rev. B **89**, 184305 (2014).

[24] P. Jobez, C. Laplane, N. Timoney, N. Gisin, A. Ferrier, P. Goldner, and M. Afzelius, Coherent Spin Control at the Quantum Level in an Ensemble-Based Optical Memory, Phys. Rev. Lett. **114**, 230502 (2015).

[25] R. M. Macfarlane, A. Arcangeli, A. Ferrier, and P. Goldner, Optical Measurement of the Effect of Electric Fields on the Nuclear Spin Coherence of Rare-Earth Ions in Solids, Phys. Rev. Lett. **113**, 157603 (2014).

[26] J. Mlynek, N. C. Wong, R. G. DeVoe, E. S. Kintzer, and B. G. Brewer, Raman Heterodyne Detection of Nuclear Magnetic Resonance, Phys. Rev. Lett. **50**, 993 (1983).

[27] N. C. Wong, E. S. Kintzer, J. Mlynek, R. G. DeVoe, and R. G. Brewer, Raman heterodyne detection of nuclear magnetic resonance, Phys. Rev. B **28**, 4993 (1983).

[28] F. Könz, Y. Sun, C. Thiel, R. Cone, R. Equall, R. Hutcheson, and R. Macfarlane, Temperature and concentration dependence of optical dephasing, spectral-hole lifetime, and anisotropic absorption in Eu^{3+}:Y_2SiO_5, Phys. Rev. B **68**, 085109 (2003).

[29] R. Yano, M. Mitsunaga, and N. Uesugi, Ultralong optical dephasing time in Eu^{3+}:Y_2SiO_5, Opt. Lett. **16**, 1884 (1991).

[30] J. Longdell, A. Alexander, and M. Sellars, Characterization of the hyperfine interaction in europium-doped yttrium orthosilicate and europium chloride hexahydrate, Phys. Rev. B **74**, 195101 (2006).

[31] R. Orbach, Spin-lattice relaxation in rare-earth salts, Proc. R. Soc. A **264**, 458 (1961).

[32] D. E. McCumber and M. D. Sturge, Linewidth and temperature shift of the R lines in ruby, J. Appl. Phys. **34**, 1682 (1963).

[33] W. B. Mims, Phase memory in electron spin echoes, lattice relaxation effects in $CaWO_4$: Er, Ce, Mn, Phys. Rev. **168**, 370 (1968).

[34] R. W. Equall, Y. Sun, R. L. Cone, and R. M. Macfarlane, Ultraslow Optical Dephasing in Eu^{3+}:Y_2SiO_5, Phys. Rev. Lett. **72**, 2179 (1994).

[35] E. Fraval, M. Sellars, and J. Longdell, Dynamic Decoherence Control of a Solid-State Nuclear-Quadrupole Qubit, Phys. Rev. Lett. **95**, 030506 (2005).

[36] E. Fraval, M. Sellars, and J. Longdell, Method of Extending Hyperfine Coherence Times in Pr^{3+}:Y_2SiO_5, Phys. Rev. Lett. **92**, 077601 (2004).